Do bifunctionalised labels solve the problem of dye diffusion in FRET analysis?

Katarzyna Walczewska-Szewc and Ben Corry

Supplementary Information

1 Spectroscopic properties of rosamine

To be able to determine FRET between two rosamine dyes the information about the Förster radius and the orientation of the emission and absorption transition moments within the molecular structure is needed. Since in this work we are more focused on the qualitative description of the influence of bifunctionalisation on FRET, without comparing our result to an experimental data, a few simplifications have been made. First, based on the analysis of structurally similar dyes[1,2], we assumed that the emission and absorption transition moments are parallel and lie roughly along the plane of the aromatic head group of each dye (Fig. B1). Secondly we assume that the absorption and emission

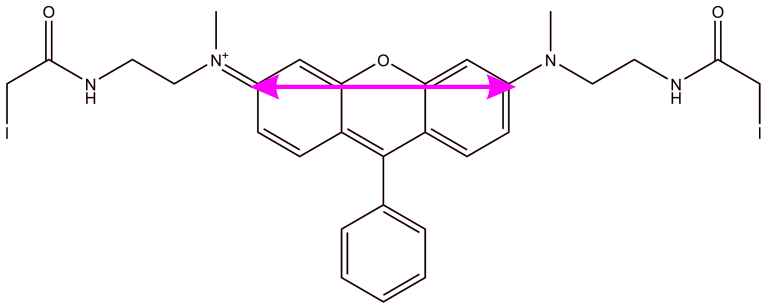

Figure B1: Assumed direction of the emission and absorption transition moment in rosamine dyes

spectra of each version of rosamine are the same. Consequently, the Förster radius that is determined based on these spectra is also the same. To determine R_0 we used information about spectra, a quantum yield and an extinction coefficient obtained by Wu & Burgess[3]. Although the derivative of rosamine from the publication (1c) is not the same as in our case, we assumed that its spectral properties are close enough to obtain an approximate value of R_0. The Förster radius (in the isotropic approximation) was calculated using following equation

$$R_0^6 = \frac{9000(\ln 10)\frac{2}{3}Q_D J}{128\pi^5 n^4 N} \tag{1}$$

where Q_D is the quantum yield of rosamine, n and N are the refractive index of water and the Avogadro constant, and

$$J = \int_0^\infty \frac{f_D(\nu)\varepsilon_A(\nu)}{\nu^4} d\nu \tag{2}$$

is the overlap integral. In here, $f_D(\nu)$ is the donors emission spectrum normalised on the wavenumber (ν) scale and $\varepsilon_A(\nu)$ is the absorption spectrum of an acceptor normalised by the molar extinction coefficient.

2 MD simulations

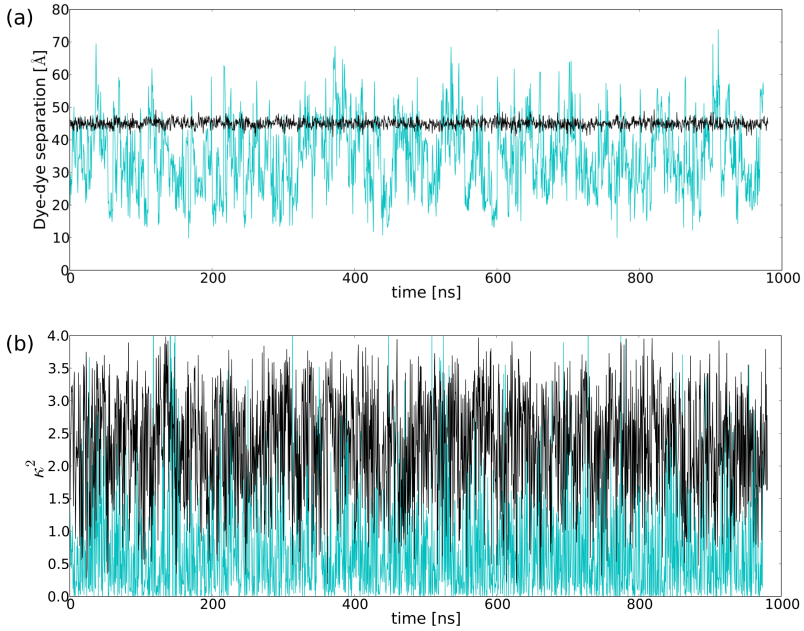

Figure B3: The time evolution of dye-dye distance (a) and orientation factor (b). The bifunctional case is shown in black, whereas the evolution of system labelled with longer version of monofunctional dyes is drawn in cyan.

For each tethering case (bifunctional dye and monofunctional dyes with short and long linker) two independent MD simulations were run for a period of 1 μs. During this time, as shown on Figure B3a, we could observe that dye-dye separation for monofunctional dyes (cyan line) changed significantly, whereas the bifunctional dyes (black line) were much less mobile.

The orientation factor (Fig. B3b) fluctuates significantly for both the mono- and bifunctional dyes, however, in the case of bifunctionalised dyes (black line) the range of κ^2 variations is slightly narrower.

The length of the MD simulations was adjusted to ensure the fair convergence of trajectories. As a main criterion we have chosen the convergence of the cumulative average of dye-dye separation and orientation factor (Fig. B2 a and b respectively). The system of protein labelled with bifunctionalised dyes reach the convergence after 100 ns of simulation, whereas, for the dyes tethered by single linker, this time extends to 500 ns for the longer label and 900 ns for the shorter one.

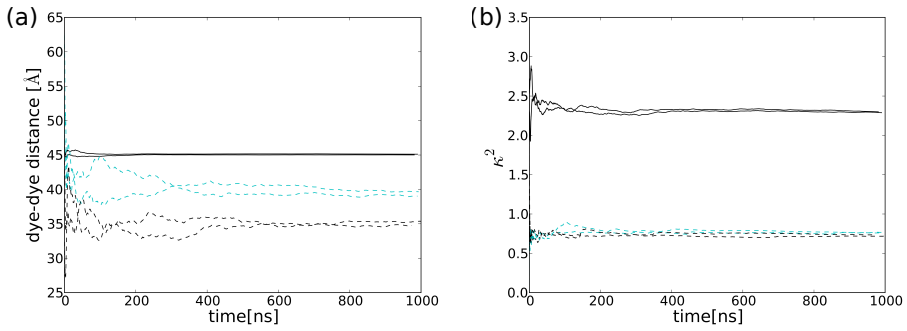

Figure B2: Cumulative average of dye-dye separation (a) and orientation factor (b) for a pair of bifunctional dyes (solid black lines), monofunctional version of dyes with shorter linker (dashed cyan lines) and longer linker (dashed black lines). Two independent MD simulations are run for each case.

The convergence of cumulative averages means that both runs of MD simulation sample the same conformational space. Hovever, it may not clearly indicate that the total conformational space is sampled enough. Therefore, to roughly check if the sampling of MD simulations is sufficient, we compared histograms of the dihedral angles with its multiplicity parameter from the MD force field. In Figure B3 the histograms of the dihedral angles for the bifunctional and longer monofunctional dyes are shown. In the bifunctional case (Fig. B3a), the values of dihedral angles are calculated separately for both linkers (cyan and black curves). For most dihedral angles, the number of maxima on the histograms is greater or equal the multiplicity parameter (shown in magenta) indicating that the dyes most likely sample all available conformations. The only possible exceptions is for dihedrals II and IV which sample a lower number of conformations than in the force field. While this may suggest that the sampling is insufficient, it may also be a result of restrained motion of the entire dye. All dihedral angles in the long monofunctional dyes undergo the transition between all possible dihedral values suggest good sampling of the dye conformations.

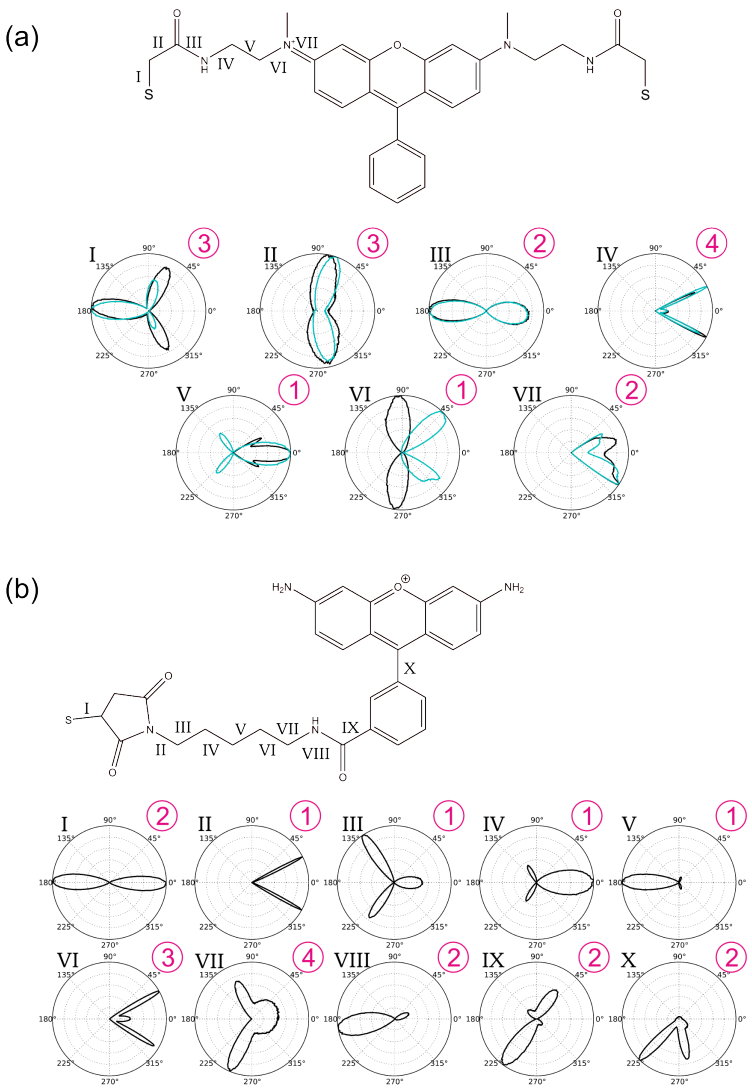

Figure B3: Histograms of the dihedral angles value obtained during MD simulation of the bifunctional (a) and monofunctional (b) dyes. Two linkers of a bifunctional dye are analysed separately and are shown as the cyan and black curves. The multiplicity of each dihedral in the force field is shown as a magenta number.

3 How much does restraint on polyproline restrict its motion?

In this work we want to focus only on the effects resulting from the dynamics of the attached dyes. Hence, to reduce the influence of the dynamics of the macromolecule, we restrained the positions of proline α carbons during the MD simulations with a harmonic potential with force constant 1 kcal/mol Å^2. The displacement of the restrained helix during simulation is shown in Fig. B4a as the composition of one hundred snapshots of the trajectory and in Fig. B4c (cyan curve) as a root square mean deviation of the polyproline atoms position from the starting position.

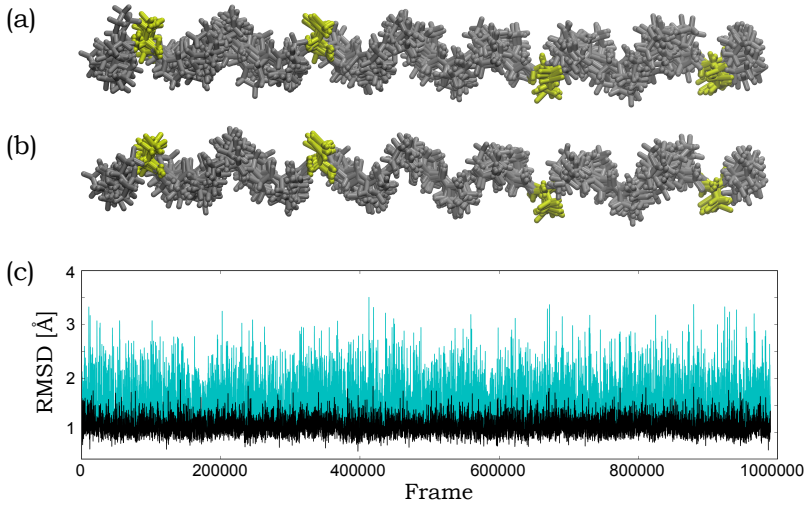

Figure B4: The displacement of the restrained polyproline chain during simulation (a). The polyproline chain after alignement (b). The root square mean deviation of the polyproline atoms position (c) before and after alignement (cyan and black curve respectively).

It can be seen, that applying this restriction effectively limits the motion of the helix. However, to reduce this effect even more we aligned all frames prior to analysis. The result of this alignment is shown in Fig. B4b and c (black curve).

4 Anisotropy decay

Measurements of fluorescence anisotropy may help to assess the so called rotational correlation time. This quantity represents timescale of rotational motion of a dye and is critical to determine in which regime FRET should be calculated.

Based on the detailed study by Schröder et al.[4] in which methods of accounting to fluorescence anisotropy in MD simulations has been presented, the anisotropy decay curve was calculated as

$$r(t) = \frac{2}{5}\langle P_2[\mu(s)\cdot\mu(s+t)]\rangle, \tag{3}$$

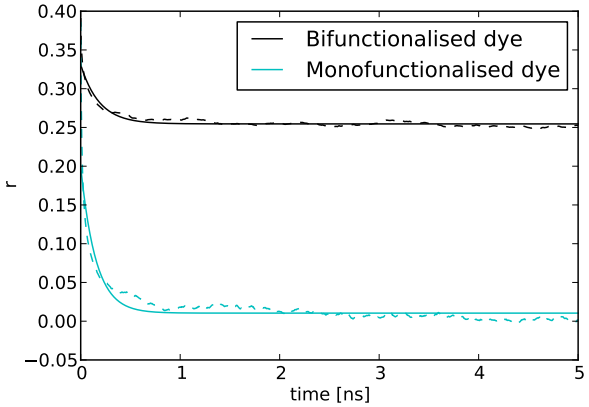

Figure B5: Fluorescence anisotropy decay for bifunctional (black) and monofunctional dye with long linker (cyan). Dashed lines represent the average decay obtained from MD simulations, whereas solid lines represent the single exponential functions fitted to the decay curves.

where $P_s(x) = (3x^2 - 1)/2$, $\mu(s)$ is a dipole of the transition moment at the time of excitation, and $\mu(s + t)$ is the same dipole after period t, during which the dye undergoes rotational diffusion. The averaged anisotropy decay was obtained with the method described previously [1]. Each single frame in the trajectory was selected as the excitation moment and the anisotropy was calculated for each t started from this frame. Then, all decays were averaged. Fitting the decay curve with a single exponential function,

$$r(t) = Ae^{-t/\tau_{rot}} + B \tag{4}$$

yields a rotational correlation time, τ_{rot}.

To determine the suitable regime of calculating FRET, the rotational correlation time needs to be compared with an average time of energy transfer (τ_{FRET}). This can be assessed based on an average transfer efficiency (E) and a lifetime of donor molecule in the absence of acceptor (τ_0),

$$E = \frac{1}{1 + \tau_{FRET}/\tau_0} \tag{5}$$

The anisotropy decay curves for bifunctional and monofunctional dye are presented in Fig. B5. Regardless on the tethering method, calculated rotational correlation times are very close (0.18 and 0.15 ns respectively). Comparing those with the average time of FRET (0.48 and 0.70 ns) may suggest that in both tethering cases the dynamic regime of FRET calculations is preferred as $\tau_{rot} < \tau_{FRET}$.

References

[1] B. A. Corry and D. Jayatilaka, *Biophys. J.*, 2008, **133**, 2711–2721.

[2] M. Sauer, J. Hofkens and J. Enderlein, *Handbook of Fluorescence Spectroscopy and Imaging: From Ensemble to Single Molecules*, Wiley, 2010.

[3] L. Wu and K. Burgess, *J. Org. Chem.*, 2008, **73**, 8711–8718.

[4] G. F. Schröder, U. Alexiev and H. Grubmüller, *Biophysical Journal*, 2005, **89**, 3757 – 3770.